Oxamato-Bridged Trinuclear $Ni^{II}Cu^{II}Ni^{II}$ Complexes with Irregular Spin State Structures and a Binuclear $Ni^{II}Cu^{II}$ Complex with an Unusual Supramolecular Structure: Crystal Structure and Magnetic Properties

En-Qing Gao,[†,‡] Jin-Kui Tang,[†] Dai-Zheng Liao,*[,†] Zong-Hui Jiang,[§] Shi-Ping Yan,[†] and Geng-Lin Wang[†]

Department of Chemistry, Nankai University, Tianjin, 300071, P. R. China, Department of Chemistry, Qufu Normal University, Qufu, 273165, P. R. China, and State Key Laboratory of Structural Chemistry, Institute of Research on Structures of Matter, Fuzhou, 350002, P. R. China

Received September 8, 2000

Four oxamato-bridged heterotrinuclear $Ni^{II}Cu^{II}Ni^{II}$ complexes of formula $\{[Ni(bispictn)]_2Cu(pba)\}(ClO_4)_2\cdot 2.5H_2O$ (**1**), $\{[Ni(bispictn)]_2Cu(pbaOH)\}(ClO_4)_2\cdot H_2O$ (**2**), $\{[Ni(cth)]_2Cu(pba)\}(ClO_4)_2$ (**3**), and $\{[Ni(cth)]_2Cu(opba)\}(ClO_4)_2\cdot H_2O$ (**4**) and a binuclear $Ni^{II}Cu^{II}$ complex of formula $[Cu(opba)Ni(cth)]\cdot CH_3OH$ (**5**) have been synthesized and characterized by means of elemental analysis, IR, ESR, and electronic spectra, where pba = 1,3-propylenebis(oxamato), pbaOH = 2-hydroxyl-1,3-propylenebis(oxamato), opba = *o*-phenylenebis(oxamato), bispictn = *N*,*N*′-bis(2-pyridylmethyl)-1,3-propanediamine, and cth = *rac*-5,7,7,12,14,14-hexamethyl-1,4,8,11-tetraazacyclotetradecane. The crystal structures of **1**, **3**, and **5** have been determined. The structures of complexes **1** and **3** consist of trinuclear cations and perchlorate anions, and that of **5** consists of neutral binuclear molecules which are connected by hydrogen bonds and $\pi-\pi$ interactions to produce a unique supramolecular "double" sheet. In the three complexes, the copper atom in a square-planar or axially elongated octahedral environment and the nickel atom in a distorted octahedral environment are bridged by the oxamato groups, with Cu···Ni separations between 5.29 and 5.33 Å. The magnetic properties of all five complexes have been investigated. The $\chi_M T$ versus T plots for **1**−**4** exhibit the minimum characteristic of antiferromagnetically coupled NiCuNi species with an irregular spin state structure and a spin-quartet ground state. The $\chi_M T$ versus T plot for **5** is typical of an antiferromagnetically coupled NiCu pair with a spin-doublet ground state. The $Ni^{II}-Cu^{II}$ isotropic interaction parameters for the five complexes were evaluated and are between 102 and 108 cm^{-1} ($\hat{H} = -J\hat{S}_{Cu}\cdot\hat{S}_{Ni}$).

Introduction

Molecular magnetism has seen a rapid development in the last two decades or so.[1−3] Particular emphasis has been placed on heterobimetallic complexes.[3,4] The magnetic interaction between two nonequivalent paramagnetic centers may lead to situations which cannot be encountered with species containing only one kind of center. For instance, the strict orthogonality of magnetic orbitals, which favors ferromagnetic interactions and stabilizes the high-spin state, is much easier to achieve in heterobimetallic species.[4] Another approach to obtain molecular species with high-spin ground states is to locate a small local spin between two large local spins (Scheme 1).[4,5] The antiferromagntic interaction between neighboring local spins will align the two large local spins in a parallel fashion, that is, the small central spin polarizes the two large terminal spins in a ferromagnetic-like fashion. The spin-state structure of such a species is irregular with $S_g = |2S_A - S_B|$ for the ground state.

Scheme 1

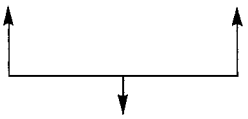

This spin topology has been achieved, for instance, in some $Mn^{II}Cu^{II}Mn^{II}$ ($S_g = {}^9/_2$),[5] $Ni^{II}Cu^{II}Ni^{II}$ ($S_g = {}^3/_2$),[5,6] and $Fe^{III}Ni^{II}$-Fe^{III} ($S_g = 4$)[7] species. The approach has been extended to species of higher nuclearity, such as an Mn^{II}_6(nitronyl nitroxide)$_6$ ring hexamer ($S_g = 12$)[8] and a cyano-bridged $Cr^{III}Mn^{II}_6$ species ($S_g = 27/2$).[9] This approach is also important for the design of ferrimagnetic chain compounds exhibiting a spontaneous magnetization.[10−16]

* To whom correspondence should be addressed. E-mail: coord@nankai.edu.cn. Fax: +86−22−23502779.
† Nankai University.
‡ Qufu Normal University.
§ Institute of Research on Structures of Matter.

(1) Kahn, O. *Molecular Magnetism*; VCH: New York, 1993.
(2) Coronado, E., Delhaès, P., Gatteschi, D., Miller, J. S., Eds. *Molecular Magnetism: From Molecular Assemblies to the Devices*; Kluwer: The Netherlands, 1996.
(3) Kahn, O. *Adv. Inorg. Chem*. **1996**, *43*, 179.
(4) Kahn, O. *Struct. Bonding (Berlin)* **1987**, *68*, 89.
(5) Pei, Y.; Journaux, Y.; Kahn, O. *Inorg. Chem*. **1988**, *27*, 399.
(6) Ribas, J.; Diaz, C.; Costa, R.; Journaux, Y.; Mathonière, C.; Kahn, O.; Gleizes, A. *Inorg. Chem.* **1990**, *29*, 2042.
(7) Chaudhuri, P.; Winter, M.; Della Vedova, B. P. C.; Fleischhauer, P.; Haase, W.; Flörke, U.; Haupt, H. J. *Inorg. Chem.* **1991**, *30*, 4777.
(8) Caneschi, A.; Gatteschi, D.; Laugier, J.; Rey, P.; Sessoli, R.; Zanchini, C. *J. Am. Chem. Soc*. **1988**, *110*, 2795.
(9) Mallah, T.; Ferlay, S.; Scuiller, A.; Verdaguer, M. In *Magnetism: A Supramolecular Function*; Kahn, O., Ed.; Kluwer: The Netherlands, 1996; p 597.
(10) Pei, Y.; Verdaguer, M.; Kahn, O.; Sletten, J.; Renard, J. *J. Am. Chem. Soc.* **1986**, *108*, 7428.
(11) Kahn, O.; Pei, Y.; Verdaguer, M.; Renard, J.; Sletten, J. *J. Am. Chem. Soc.* **1988**, *110*, 782.
(12) Nakatani, K.; Carriat, J. Y.; Journaux, Y.; Kahn, O.; Lloret, F.; Renard, J. P.; Pei, Y.; Verdaguer, M. *J. Am. Chem. Soc.* **1989**, *111*, 5739.

10.1021/ic001023h CCC: $20.00 © 2001 American Chemical Society
Published on Web 05/18/2001

Chart 1

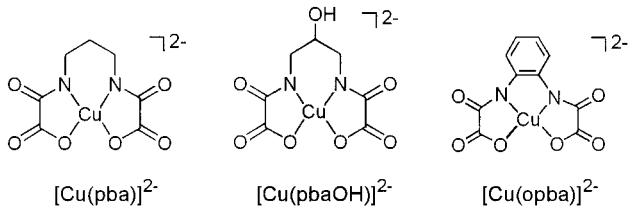

To obtain the desired spin topology, chemists have to design and synthesize a species with a specific molecular topology. One of the best strategies is the "complex as ligand" approach, i.e., using as precursors mononuclear complexes that contain potential donors for another metal ion.[3,4,17−19] A good example is represented by the use of mononuclear *N*,*N*′-substituted bis(oxamato)−copper(II) complexes such as $[Cu(pba)]^{2-}$, $[Cu(pbaOH)]^{2-}$, and $[Cu(opba)]^{2-}$ (Chart 1). These anionic precursors are particularly suitable for designing heterotrinuclear complexes and heterobimetallic chain compounds and have played an important role in the development of molecular magnetism.[3] For instance, the oxamato-bridged chain compound $[MnCu(pbaOH)(H_2O)_3]$ is one of the first genuine molecular-based magnets,[10,11] and an $Mn^{II}Cu^{II}Mn^{II}$ and an $Ni^{II}Cu^{II}Ni^{II}$ species derived from $[Cu(pba)]^{2-}$ have provided the first examples of trinuclear complexes that exhibit irregular spin state structures and demonstrated the antiferromagnetic approach to design high-spin species.[5] So far, a number of oxamato-bridged heterobimetallic complexes of ABA type have been reported.[5,6,20−22] However, to our knowledge, only one species, $\{[Ni(bapa)(H_2O)]_2Cu(pba)\}(ClO_4)_2$ [bapa = bis(3-aminopropyl)-amine], has been characterized by X-ray crystallography.[6]

In this paper, we report the synthesis and magnetic and spectroscopic properties of four oxamato-bridged $Ni^{II}Cu^{II}Ni^{II}$ species. Their formulas are $\{[Ni(bispictn)]_2Cu(pba)\}(ClO_4)_2 \cdot 2.5H_2O$ (**1**), $\{[Ni(bispictn)]_2Cu(pbaOH)\}(ClO_4)_2 \cdot H_2O$ (**2**), $\{[Ni(cth)]_2Cu(pba)\}(ClO_4)_2$ (**3**), and $\{[Ni(cth)]_2Cu(opba)\}(ClO_4)_2 \cdot H_2O$ (**4**), where bispictn = *N*,*N*′-bis(2-pyridylmethyl)-1,3-propanediamine and cth = *rac*-5,7,7,12,14,14-hexamethyl-1,4,8,11-tetraazacyclotetradecane (Chart 2). The crystal structures of **1** and **3** were determined. The magnetic properties of **3**, one of the first bis(oxamato)-bridged trinuclear species, has been reported by Kahn et al.,[5] but the X-ray structural results were not available. In the course of synthesizing **4**, we obtained the crystals of another complex, namely, the neutral binuclear species $[Cu(opba)Ni(cth)] \cdot CH_3OH$ (**5**). To our knowledge, only one oxamato-bridged binuclear complex, $\{[Ni(bapa)(H_2O)]Cu(pba)\} \cdot 2H_2O$, has been reported in the literature, and its structure has not yet been determined.[6] Complex **5** exhibits a unique supramolecular structure formed via hydrogen bonds and $\pi-\pi$ interactions. Its magnetic properties are also described here.

Chart 2

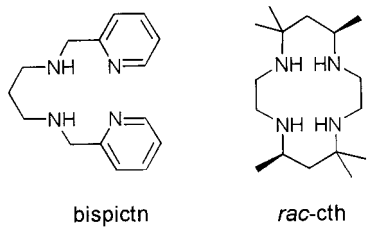

Experimental Section

Materials and Synthesis. All the starting chemicals were of A. R. grade and used as received. The mononuclear precursors, $Na_2[Cu(pba)] \cdot 6H_2O$,[23] $Na_2[Cu(pbaOH)] \cdot 3H_2O$,[11] $Na_2[Cu(opba)] \cdot 3H_2O$,[16] $[Ni(cth)](ClO_4)_2$,[24] and $[Ni(bispictn)](ClO_4)_2 \cdot H_2O$,[25,26] were prepared as described in the literature.

$\{[Ni(bispictn)]_2Cu(pba)\}(ClO_4)_2 \cdot 2.5H_2O$ (1). To a stirred aqueous solution (8 cm^3) of $[Ni(bispictn)](ClO_4)_2 \cdot H_2O$ (0.4 mmol) was added dropwise an aqueous solution (5 cm^3) of $[Cu(pba)] \cdot 6H_2O$ (0.2 mmol). The mixture was stirred at room temperature for 10 min and then filtered. Slow evaporation of the filtrate afforded violet blue microcrystals in 2 weeks. The product was filtered out, washed with ethanol, and dissolved in an acetonitrile/water mixture (1:1). Slow evaporation of the solution at room temperature afforded red crystals. Anal. Calcd for $C_{37}H_{51}Cl_2CuN_8Ni_2O_{16.50}$: C, 38.59; H, 4.46; N, 12.16. Found: C, 38.75; H, 4.26; N, 12.36. Main IR bands (KBr, cm^{-1}): 3450m (br), 3240s, 2900m, 1600vs (br), 1480m, 1435s, 1352m, 1312s, 1285w, 1080vs (br), 1015m, 895w, 790m, 760s.

$\{[Ni(bispictn)]_2Cu(pbaOH)\}(ClO_4)_2 \cdot H_2O$ (2). The complex was prepared in the same way as **1**, using $[Cu(pbaOH)] \cdot 3H_2O$ instead of $[Cu(pba)] \cdot 6H_2O$, but our efforts to grow single crystals failed. Anal. Calcd for $C_{37}H_{48}Cl_2CuN_8Ni_2O_{16}$: C, 38.95; H, 4.24; N, 12.28. Found: C, 38.56; H, 4.34; N, 12.17. Main IR bands (KBr, cm^{-1}): 3420s (br), 3290s, 2920m, 1605vs (br), 1482m, 1440s, 1360w, 1325s, 1290m, 1085vs (br), 1020m, 900w, 792w, 760s.

$\{[Ni(cth)]_2Cu(pba)\}(ClO_4)_2$ (3). Blue crystals of **3** were obtained by slow diffusion between an aqueous solution (10 cm^3) of $[Cu(pba)] \cdot 6H_2O$ (0.3 mmol) and a solution of $[Ni(cth)](ClO_4)_2$ (0.6 mmol) in a 1:1 acetonitrile/methanol mixture (10 cm^3) in an H-shaped tube. Anal. Calcd for $C_{39}H_{78}Cl_2CuN_{10}Ni_2O_{14}$: C, 40.28; H, 6.76; N, 12.04. Found: C, 40.16; H, 6.58; N, 11.76. Main IR bands (KBr, cm^{-1}): 3250m, 2950m, 1600s (br), 1440m, 1365m, 1320m, 1270m, 1165m, 1080s (br), 1025sh, 955m, 855w, 820w, 793m, 770w.

$\{[Ni(cth)]_2Cu(opba)\}(ClO_4)_2 \cdot H_2O$, 4 and $[Cu(opba)Ni(cth)] \cdot CH_3OH$ (5). Slow diffusion between an aqueous solution of $[Cu(opba)] \cdot 3H_2O$ and a solution of $[Ni(cth)](ClO_4)_2$ in acetonitrile/methanol also afforded blue crystals. The IR spectrum of this sample indicates the presence of perchlorate ions, but the X-ray crystallographic analysis for one of the crystals revealed the structure of the binuclear species **5**. Therefore, the sample thus obtained is a mixture of the bi- and trinuclear species.

To obtain a pure sample of the trinuclear species **4**, an aqueous solution (10 cm^3) of $[Cu(opba)] \cdot 3H_2O$ (0.3 mmol) was added dropwise to a continuously stirred solution of $[Ni(cth)](ClO_4)_2$ (0.61 mmol) in acetonitrile/methanol (1:1, 15 cm^3). The mixture was stirred for 10 min and then filtered. The filtrate was allowed to evaporate at room temperature, precipitating out blue microcrystals in about 3 weeks. The product was filtered out and dried in air. We have not been able to get single crystals suitable for X-ray diffraction. Anal. Calcd for $C_{42}H_{78}Cl_2CuN_{10}Ni_2O_{15}$: C, 41.52; H, 6.47; N, 11.53. Found: C, 41.34; H,

(13) Nakatani, K.; Bergerat, P.; Codjovi, E.; Mathonière, C.; Pei, Y.; Kahn, O. *Inorg. Chem.* **1991**, *30*, 3977.
(14) Baron, V.; Gillon, B.; Sletten, J.; Renard, J. P.; Mathonière, C.; Codjovi, E.; Kahn, O. *Inorg. Chim. Acta* **1995**, *235*, 69.
(15) Caneschi, A.; Gatteschi, D.; Renard, J. P.; Rey, P.; Sessoli, R. *J. Am. Chem. Soc.* **1989**, *111*, 785.
(16) Stumpf, H. O.; Pei. Y.; Kahn, O.; Sletten, J.; Renard, J. P. *J. Am. Chem. Soc.* **1993**, *115*, 6738.
(17) Gruber, S. J.; Harris, C. M.; Sinn, E. *J. Inorg. Nucl. Chem.* **1968**, *30*, 1805.
(18) O'Brien, N. B.; Maier, T. O.; Paul, I. C.; Drago, R. S. *J. Am. Chem. Soc.* **1973**, *95*, 6640.
(19) Ojima, H.; Nonoyama, K. *Coord. Chem. Rev.* **1988**, *92*, 85.
(20) Vicente, R.; Escuer, A.; Ribas, J. *Polyhedron* **1992**, *11*, 857.
(21) Miao, M.-M.; Cheng, P.; Liao, D.-Z,; Jiang, Z.-H.; Wang, G.-L. *Chin. Sci. Bull.* **1996**, *41*, 995.
(22) Miao, M.-M.; Cheng, P.; Liao, D.-Z,; Jiang, Z.-H.; Wang, G.-L. *Transition Met. Chem.* **1997**, *22*, 19.
(23) Nonoyama, K.; Ojima, H.; Nonoyama, M. *Inorg. Chim. Acta* **1976**, *20*, 127.
(24) Tait, A. M.; Bush, D. H. *Inorg. Synth.* **1978**, *18*, 10.
(25) Che, C.-M.; Tang, W.-T.; Li, C.-H. *J. Chem. Soc., Dalton Trans.* **1990**, 3735.
(26) Gibson, J. G.; Mckenzie, E. D. *J. Chem. Soc. A* **1971**, 1666.

Table 1. Summary of Crystallographic Data for Complexes **1**, **3**, and **5**

	1	**3**	**5**
formula	$C_{37}H_{51}Cl_2CuN_{10}Ni_2O_{16.50}$	$C_{39}H_{78}Cl_2CuN_{10}Ni_2O_{14}$	$C_{27}H_{44}N_6O_7CuNi$
fw	1151.74	1162.97	686.93
space group	$P\bar{1}$	$Pna2_1$	$P2_1/n$
a, Å	11.7769(18)	35.376(4)	12.159(4)
b, Å	13.955(2)	10.7433(11)	15.210(5)
c, Å	18.041(3)	14.3949(14)	17.271(6)
α, deg	101.071(3)		
β, deg	103.473(3)		90.622(7)
γ, deg	114.277(3)		
V, Å^3	2486.0(7)	5470.8(10)	3193.8(19)
Z	2	4	4
ρ_{calcd}, g/cm^3	1.539	1.412	1.429
μ(Mo Kα), mm^{-1}	1.357	1.230	1.307
T, K	293(2)	298(2)	293(2)
R1[a] [$I > 2\sigma(I)$]	0.0629	0.0623	0.0508
wR2[b] [$I > 2\sigma(I)$]	0.1489	0.1294	0.1287

[a] $R1 = \sum||F_o| - |F_c||/\sum|F_o|$. [b] $wR2 = \{\sum[w(F_o^2 - F_c^2)^2]/\sum[w(F_o^2)^2]\}^{1/2}$.

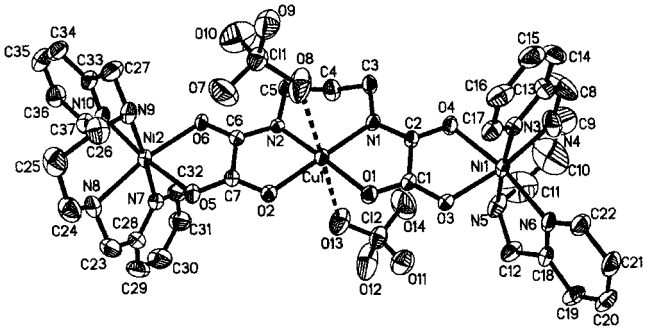

Figure 1. ORTEP view of the trinuclear complex in **1**. The thermal ellipsoids are drawn at the 30% probability level.

6.31; N, 11.36. Main IR bands (KBr, cm^{-1}): 3400w, 3250m, 2950m, 1610s (br), 1450m, 1355m, 1270w, 1165m, 1080s (br), 1030sh, 950m, 865m, 820w, 780w, 750w.

To obtain a pure sample of **5**, a methanol solution (20 cm^3) of [Ni(cth)](ClO$_4$)$_2$ (0.34 mmol) was added dropwise to a continuously stirred aqueous solution (10 cm^3) of Na$_2$[Cu(opba)]·3H$_2$O (0.35 mmol). The binuclear species precipitated as a blue microcrystalline powder, which was filtered off, washed with methanol, and dried in air. Anal. Calcd for $C_{27}H_{44}CuN_6NiO_7$: C, 47.21; H, 6.46; N, 12.23. Found: C, 46.97; H, 6.21; N, 12.44. Main IR bands (KBr, cm^{-1}): 3370m, 3170m, 2950m, 1600vs (br), 1455s, 1400m, 1340m, 1270s, 1165s, 1025m, 950w, 865m, 810w, 780s, 755s.

Physical Measurements. Elemental analyses (C, H, N) were performed on a Perkin-Elmer 240 analyzer. IR spectra were recorded on a Shimadzu IR-408 spectrometer as KBr pellets, electronic spectra on a Shimadzu UV-365 UV−vis−near-IR recording spectrophotometer in acetonitrile, and X-band ESR spectra on a Bruker ER 200 D-SRC ESR spectrometer. Variable-temperature magnetic susceptibilities were measured on a Quantum Design MPMS-7 SQUID magnetometer. Diamagnetic corrections were made with Pascal's constants for all the constituent atoms.[27]

Crystallographic Studies. Diffraction intensity data for single crystals of **1**, **3**, and **5** were collected at room temperature on a Bruker Smart 1000 CCD area detector equipped with graphite-monochromated Mo Kα radiation ($\lambda = 0.71073$ Å). Empirical absorption corrections were applied using the SADABS program. The structure was solved by the direct method and refined by the full-matrix least-squares method on F^2 with anisotropic thermal parameters for all non-hydrogen atoms.[28] One of the water molecules in **1** is disordered, and an occupancy factor of 0.5 was assumed for each of the two positions. The hydrogen atoms of solvent molecules were not added, and the other hydrogen atoms were located geometrically and refined isotropically.

Pertinent crystallographic data and structure refinement parameters are summarized in Table 1.

Table 2. Selected Bond Distances (Å) and Angles (deg) for **1**

Cu(1)−N(2)	1.931(5)	Cu(1)−N(1)	1.934(5)
Cu(1)−O(2)	1.964(4)	Cu(1)−O(1)	1.981(4)
Ni(1)−N(4)	2.067(7)	Ni(1)−O(3)	2.077(4)
Ni(1)−N(3)	2.087(6)	Ni(1)−N(6)	2.087(5)
Ni(1)−N(5)	2.089(6)	Ni(1)−O(4)	2.093(4)
Ni(2)−O(6)	2.065(4)	Ni(2)−N(7)	2.077(6)
Ni(2)−N(8)	2.091(6)	Ni(2)−N(10)	2.098(6)
Ni(2)−O(5)	2.116(5)	Ni(2)−N(9)	2.118(7)
O(1)−C(1)	1.256(7)	O(3)−C(1)	1.257(7)
O(4)−C(2)	1.268(7)	N(1)−C(2)	1.296(7)
C(1)−C(2)	1.530(9)	C(6)−C(7)	1.544(9)
O(2)−C(7)	1.278(7)	O(5)−C(7)	1.252(7)
O(6)−C(6)	1.270(7)	N(2)−C(6)	1.295(8)
N(2)−Cu(1)−N(1)	96.6(2)	N(2)−Cu(1)−O(2)	85.0(2)
N(1)−Cu(1)−O(2)	177.7(2)	N(2)−Cu(1)−O(1)	176.1(2)
N(1)−Cu(1)−O(1)	84.30(19)	O(2)−Cu(1)−O(1)	94.27(18)
N(4)−Ni(1)−O(3)	169.1(3)	N(4)−Ni(1)−N(3)	80.0(3)
O(3)−Ni(1)−N(3)	91.9(2)	N(4)−Ni(1)−N(6)	96.4(3)
O(3)−Ni(1)−N(6)	91.83(19)	N(3)−Ni(1)−N(6)	97.5(2)
N(4)−Ni(1)−N(5)	96.5(3)	O(3)−Ni(1)−N(5)	91.9(2)
N(3)−Ni(1)−N(5)	175.7(2)	N(6)−Ni(1)−N(5)	80.3(2)
N(4)−Ni(1)−O(4)	91.8(3)	O(3)−Ni(1)−O(4)	81.02(16)
N(3)−Ni(1)−O(4)	91.47(19)	N(6)−Ni(1)−O(4)	168.7(2)
N(5)−Ni(1)−O(4)	91.2(2)	O(6)−Ni(2)−N(7)	93.1(2)
O(6)−Ni(2)−N(8)	169.9(2)	N(7)−Ni(2)−N(8)	79.0(3)
O(6)−Ni(2)−N(10)	93.7(2)	N(7)−Ni(2)−N(10)	96.6(2)
N(8)−Ni(2)−N(10)	93.4(2)	O(6)−Ni(2)−O(5)	81.44(17)
N(7)−Ni(2)−O(5)	91.9(2)	N(8)−Ni(2)−O(5)	92.5(2)
N(10)−Ni(2)−O(5)	170.5(2)	O(6)−Ni(2)−N(9)	90.3(2)
N(7)−Ni(2)−N(9)	176.4(2)	N(8)−Ni(2)−N(9)	97.8(3)
N(10)−Ni(2)−N(9)	81.9(2)	O(5)−Ni(2)−N(9)	89.8(2)

Results and Discussion

Description of the Structure of 1. The structure of complex **1** consists of heterotrinuclear {[Ni(bispictn)]$_2$Cu(pba)}$^{2+}$ cations, water molecules, and two sets of weakly coordinated perchlorate ions. A perspective view of the trinuclear cation with the weakly coordinated perchlorate ion is depicted in Figure 1, and selected bond lengths and angles are listed in Table 2.

In the trinuclear cation, the copper atom and nickel atoms are bridged by oxamato groups. The copper atom is ligated by the two deprotonated amido nitrogens and the two carboxylato oxygens from the pba^{4-} ligand with a slightly distorted square-planar geometry. The deviations of the four donor atoms from the their mean plane are ±0.084 Å, and the copper atom is 0.018 Å out of the plane. The Cu−N distances (av 1.932 Å) is significantly shorter than the Cu−O ones (av 1.972 Å),

(27) Selwood, P. W. *Magnetochemistry*; Interscience: New York, 1956; p 78.
(28) Sheldrick, G. M. *SHELXS-97* and *SHELXL-97, Software for Crystal Structure Analysis*; Siemens Analytical X-ray Instruments Inc.: Madison, WI, 1997.

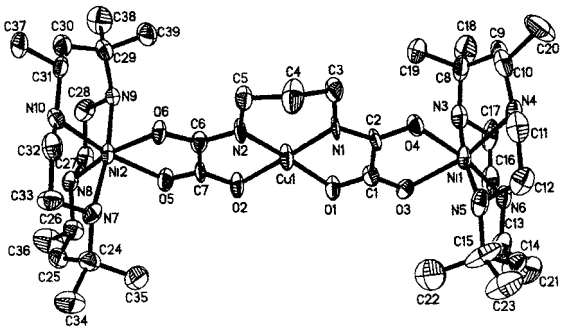

Figure 2. ORTEP view of the trinuclear cation in **3**. The thermal ellipsoids are drawn at the 30% probability level.

consistent with the greater basicity of the deprotonated amido group. Two perchlorate ions reside between the two terminal ligands, below and above the CuN_2O_2 plane, respectively. The Cu−O (perchlorate) distances are 2.845 and 2.959 Å. Therefore, the coordination polyhedron of the Cu(II) ion can be described as an octahedron with significant axial elongation (4 + 2). The nickel atom is in a distorted octahedral environment. The equatorial positions are occupied by two carbonyl oxygen atoms arising from $[Cu(pba)]^{2-}$ and one secondary amino nitrogen and one pyridyl nitrogen from bispictn. The two remaining positions are occupied by the other two nitrogen atoms of the terminal ligand. While both nickel atoms reside in the equatorial N_2O_2 mean planes within experimental error, the equatorial donor atoms around each nickel atom are deviated from their mean plane by ±0.134(3)−0.154(3) Å for Ni1 and ±0.133(3)−0.149(3) Å for Ni2, thus resulting in a tetrahedrally distorted equatorial environment around nickel atoms. The dihedral angles between the equatorial planes around the copper and nickel atoms are 12.8° for the Cu1−Ni1 pair and 6.1° for the Cu2−Ni2 pair. Cu1 and Ni1 are displaced toward opposite sides of the $N_2C_2O_2$ bridge plane between them by 0.176(6) and −0.026(6) Å, respectively. Cu1 and Ni2 are also displaced toward opposite sides of the bridge plane between them, by −0.117(6) and 0.131(6) Å, respectively. Both Cu···Ni distances (Cu1···Ni1 and Cu1···Ni2) through oxamato bridges are 5.296 Å.

Description of the Structure of 3. The structure of complex **3** consists of heterotrinuclear $\{[Ni(cth)]_2Cu(pba)\}^{2+}$ cations and noncoordinated perchlorate ions. A perspective view of the trinuclear cation is depicted in Figure 2, and selected bond lengths and angles are listed in Table 3.

The copper atom is in a slightly distorted square-planar environment, also with the Cu−N (deprotonated amido) distances (av 1.906 Å) being significantly shorter than the Cu−O (carboxylato) ones (av 1.954 Å). The four donor atoms are deviated from their mean plane by ±0.070−0.075 Å, and the copper atom is displaced out of the plane by 0.061 Å. The nickel atom is in a distorted octahedral environment, ligated by two carbonyl oxygen atoms arising from $[Cu(pba)]^{2-}$ and four secondary amino nitrogens from the tetraazamacrocyclic ligand. Each nickel atom resides in the equatorial N_2O_2 mean plane within experimental error. The equatorial donor atoms around nickel atoms are deviated from the mean plane by ±0.028(4)−0.035(5) Å for Ni1 and ±0.073(4)−0.093(5) Å for Ni2. The dihedral angles between the equatorial planes around the copper and nickel atoms are 7.2° for the Cu1−Ni1 pair and 8.9° for the Cu2−Ni2 pair. Cu1 and Ni1 are separated by 5.312 Å and displaced toward opposite sides of the bridge plane between them by 0.028(11) and −0.032(11) Å, respectively. Cu1 and Ni2 are separated by 5.291 Å and displaced toward the same side of the bridge plane by 0.095(11) and 0.074(11) Å, respectively.

Table 3. Selected Bond Distances (Å) and Angles (deg) for **3**

Cu(1)−N(1)	1.896(8)	Cu(1)−N(2)	1.917(9)
Cu(1)−O(2)	1.951(7)	Cu(1)−O(1)	1.957(8)
Ni(1)−O(4)	2.062(7)	Ni(1)−N(6)	2.094(9)
Ni(1)−N(4)	2.102(9)	Ni(1)−N(5)	2.135(10)
Ni(1)−O(3)	2.152(8)	Ni(1)−N(3)	2.153(10)
Ni(2)−N(8)	2.072(8)	Ni(2)−O(6)	2.074(7)
Ni(2)−N(10)	2.113(8)	Ni(2)−O(5)	2.117(8)
Ni(2)−N(7)	2.157(8)	Ni(2)−N(9)	2.163(8)
O(1)−C(1)	1.243(12)	O(3)−C(1)	1.238(12)
N(1)−C(2)	1.315(12)	O(4)−C(2)	1.277(11)
O(2)−C(7)	1.264(11)	O(5)−C(7)	1.219(11)
N(2)−C(6)	1.308(13)	O(6)−C(6)	1.273(11)
C(1)−C(2)	1.542(14)	C(6)−C(7)	1.506(14)
N(1)−Cu(1)−N(2)	93.3(3)	N(1)−Cu(1)−O(2)	178.6(4)
N(2)−Cu(1)−O(2)	85.5(3)	N(1)−Cu(1)−O(1)	84.5(3)
N(2)−Cu(1)−O(1)	171.8(5)	O(2)−Cu(1)−O(1)	96.8(3)
O(4)−Ni(1)−N(6)	170.5(3)	O(4)−Ni(1)−N(4)	87.2(3)
N(6)−Ni(1)−N(4)	101.5(4)	O(4)−Ni(1)−N(5)	87.6(4)
N(6)−Ni(1)−N(5)	89.5(4)	N(4)−Ni(1)−N(5)	84.7(4)
O(4)−Ni(1)−O(3)	80.5(3)	N(6)−Ni(1)−O(3)	91.2(3)
N(4)−Ni(1)−O(3)	166.5(3)	N(5)−Ni(1)−O(3)	100.0(4)
O(4)−Ni(1)−N(3)	99.3(3)	N(6)−Ni(1)−N(3)	84.5(4)
N(4)−Ni(1)−N(3)	90.9(4)	N(5)−Ni(1)−N(3)	171.7(4)
O(3)−Ni(1)−N(3)	85.8(3)	N(8)−Ni(2)−O(6)	168.0(3)
N(8)−Ni(2)−N(10)	102.6(4)	O(6)−Ni(2)−N(10)	89.2(3)
N(8)−Ni(2)−O(5)	89.3(3)	O(6)−Ni(2)−O(5)	78.8(3)
N(10)−Ni(2)−O(5)	168.0(3)	N(8)−Ni(2)−N(7)	90.2(3)
O(6)−Ni(2)−N(7)	89.0(3)	N(10)−Ni(2)−N(7)	84.0(4)
O(5)−Ni(2)−N(7)	97.2(3)	N(8)−Ni(2)−N(9)	85.5(3)
O(6)−Ni(2)−N(9)	96.5(3)	N(10)−Ni(2)−N(9)	90.9(3)
O(5)−Ni(2)−N(9)	88.9(3)	N(7)−Ni(2)−N(9)	172.5(3)

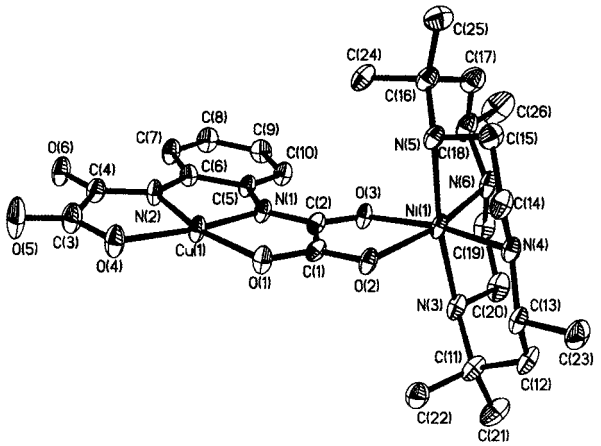

Figure 3. ORTEP view of the binuclear molecule in **5**. The thermal ellipsoids are drawn at the 30% probability level.

Description of the Structure of 5. The structure consists of neutral heterobinuclear molecules, $[Cu(opba)Ni(rac\text{-}cth)]^{2+}$, and hydrogen-bonded methanol molecules. A perspective view of the binuclear unit is depicted in Figure 3, and selected bond lengths and angles are listed in Table 4.

The copper atom resides in a slightly distorted square-planar environment. The deviations of donor atoms from the N_2O_2 mean plane are ±0.041 Å for N1 and N2 and ±0.032 Å for O1 and O4, the copper atom being 0.035 Å out of the plane. As has been observed for **1** and **3**, the Cu−N (deprotonated amido) distances (av 1.900 Å) are significantly shorter than the Cu−O (carboxylato) ones (av 1.967 Å). The whole [Cu(opba)] moiety is quite flat: the dihedral angles between the CuN_2O_2 mean plane and the phenyl ring and the O1−O2−C1−C2−N1−O3 and the O4−O5−C4−C3−N2−O6 bridge planes are only 3.8°, 4.2°, and 2.0°, respectively, and deviations from the least-squares plane defined by N1, N2, O1, O4, Cu1, and all the carbon atoms

Table 4. Selected Bond Distances (Å) and Angles (deg) for **5**

Cu(1)−N(2)	1.899(4)	Cu(1)−N(1)	1.901(3)
Cu(1)−O(1)	1.990(3)	Cu(1)−O(4)	1.944(3)
Ni(1)−O(2)	2.149(3)	Ni(1)−O(3)	2.074(3)
Ni(1)−N(3)	2.141(4)	Ni(1)−N(4)	2.086(3)
Ni(1)−N(5)	2.163(4)	Ni(1)−N(6)	2.105(4)
O(1)−C(1)	1.268(5)	O(2)−C(1)	1.240(5)
O(3)−C(2)	1.250(5)	N(1)−C(2)	1.303(5)
C(1)−C(2)	1.542(6)	O(4)−C(3)	1.297(5)
O(5)−C(3)	1.207(5)	O(6)−C(4)	1.245(5)
N(2)−C(4)	1.319(5)	C(3)−C(4)	1.556(6)
N(1)−Cu(1)−O(1)	83.90(12)	N(1)−Cu(1)−O(4)	167.85(13)
N(1)−Cu(1)−N(2)	83.25(13)	N(2)−Cu(1)−O(1)	166.45(13)
N(2)−Cu(1)−O(4)	84.61(13)	O(4)−Cu(1)−O(1)	108.25(12)
O(3)−Ni(1)−O(2)	78.87(11)	O(3)−Ni(1)−N(3)	87.95(13)
O(3)−Ni(1)−N(4)	168.68(13)	O(3)−Ni(1)−N(6)	89.58(12)
N(4)−Ni(1)−N(6)	101.50(13)	N(4)−Ni(1)−N(3)	90.79(14)
N(6)−Ni(1)−N(3)	84.44(15)	N(4)−Ni(1)−O(2)	90.30(12)
N(6)−Ni(1)−O(2)	167.30(12)	N(3)−Ni(1)−O(2)	100.23(14)
O(3)−Ni(1)−N(5)	97.92(13)	N(4)−Ni(1)−N(5)	84.54(13)
N(6)−Ni(1)−N(5)	89.95(15)	N(3)−Ni(1)−N(5)	171.86(14)
O(2)−Ni(1)−N(5)	86.49(13)		

in the moiety are in the 0.014−0.086 Å range. These data indicate the presence of an extended π conjugating system in the [Cu(opba)] moiety. The coordination environment of the nickel atom in **5** is similar to that in **3**. The equatorial donor atoms around Ni1 are deviated from the mean plane by ±0.063(2)−0.078(2) Å. The dihedral angle between the equatorial NiN_2O_2 and CuN_2O_2 mean planes is 14.8°. Cu1 and Ni1 are separated by 5.328 Å and displaced toward the same side of the bridge plane by 0.053(4) and 0.322(4) Å. As can been seen from Table 4, the C1−O2 and Cu1−O1 distances are significantly longer than C3−O5 and Cu1−O4, respectively, while the C1−O1 distance is appreciably shorter than C3−O4. These differences are consistent with the bridging and nonbridging coordination modes of the two CO_2^- carboxylato groups. However, the two amido groups, N1C2O3 and N2C4O6, show no appreciable differences within experimental error.

Complex **5** shows an interesting supramolecular structure in the lattice. The two "free" carboxylato oxygens are involved in hydrogen bonding. O6 is hydrogen-bonded to a methanol molecule with O6···O7 = 2.736 Å, while O5 is bonded to a secondary amino group arising from an adjacent binuclear molecule generated by an *n*-glide operation, with O5···N4a ($x + {}^1/_2$, $-y + {}^1/_2$, $z - {}^1/_2$) = 2.916 Å and ∠O5···H−N4a = 167.8°. The latter hydrogen bond interlinks the binuclear complex molecules to produce an infinite zigzag chain that runs along the [10$\bar{1}$] direction. The shortest intermolecular Cu···Ni distance within the chain is 6.38 Å.

Further investigation reveals that there are $\pi-\pi$ interactions between neighboring chains. Two neighboring $[Cu(opba)]^{2-}$ moieties related by inversion centers (symmetry code: $-x, -y + 1, -z + 2$) are separated by 3.35 Å (interplane distance), indicating an overlap between their π conjugating systems that are extended to the CuN_2O_2 chromophores, although the two phenyl rings do not overlap. The Cu···Cu distance is 5.84 Å. These $\pi-\pi$ interactions between neighboring chains result in an unusual quasi-2D supramolecular "double" sheet that extends along the ⟨101⟩ plane. The hydrogen-bonded methanol molecules lie between sheets.

IR and Electronic Spectra

The IR spectra of the trinuclear species **1**−**4** exhibit a sharp medium band at ca. 3250 or 3300 cm^{-1} and a broad strong band at ca. 1080 cm^{-1}, characteristic of the NH group in *rac*-cth or bispictn and the perchlorate ion, respectively. The binuclear species **5** does not exhibit any band attributable to perchlorate ions, while the ν(NH) band appears at 3170 cm^{-1}. The broad strong band at ca. 1600 cm^{-1}, which is observed in all complexes, is attributed to the ν(C═O) vibrations of the oxamato groups.[29]

Table 5. ESR and Electronic Spectral Data

complex	λ_{max}, nm (ϵ, M^{-1} cm^{-1})	*g*
1	305 (3530), 565 (208), 850 (38)	2.10, 5.44
2	310 (3910), 570 (166), 850 (52)	*a*
3	315 (1960), 570 (183), 960 (60)	*a*
4	325 (20800), 587 (250), 925 (63)	2.07, 5.40
5	328 (19900), 585 (203), 980 (88)	2.20, 5.55

[a] Not measured.

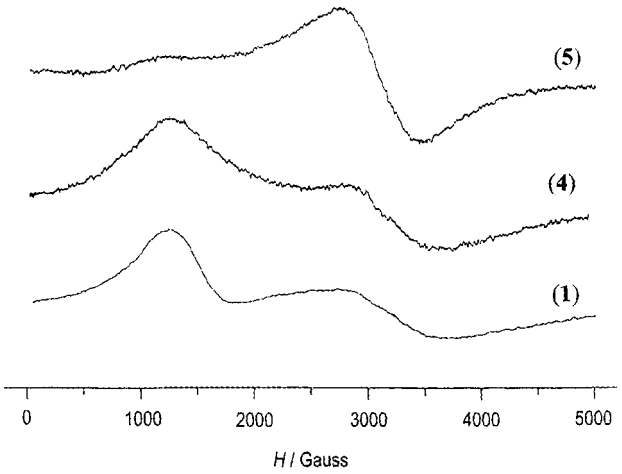

Figure 4. Polycrystalline X-band ESR spectra of complexes **1**, **4**, and **5** at room temperature.

The electronic absorption spectra of the five complexes were measured in acetonitrile solutions. Relevant data are collected in Table 5. All complexes exhibit very intense bands in the 300−325 nm region, assignable to charge-transfer transitions in the Cu(II) chromophores and/or intraligand $\pi-\pi^*$ interactions. In the 500−1000 nm region, they all exhibit two broad bands: (i) They exhibit a weak near-infrared absorption at 850 nm for **1** and **2**, and 925−980 nm for **3**−**5**. This band is due to the $^3A_2$(Ni) → $^3T_2$(Ni) transitions, assuming an O_h site symmetry for Ni(II). The blue shift of this band for **1** or **2** relative to those for the other three complexes reflects that a stronger ligand field is associated with the pyridyl donors in the bispictn ligand, which forms M → Lπ^* back-donating π bonds with Ni(II) ions. (ii) They exhibit a relatively stronger band centered at 565−590 nm, attributed to the envelope of two spin-allowed d−d transitions: $^2B_2$(Cu) → $^2B_1$(Cu) and $^3A_2$(Ni) → $^3T_1$(Ni). Because the d−d absorption of Ni(II) in an octahedral environment is usually weaker than that of Cu(II) in a tetragonal environment, this band may be dominated by the former transition. In addition, complexes **3** exhibits a very weak band at around 796 nm, attributable to the spin-forbidden transition $^3A_2$(Ni) → ^1E(Ni), which is activated by an exchange mechanism.[30,31]

ESR Spectra

The polycrystalline X-band ESR spectra of **1**, **4**, and **5** at room temperature are shown in Figure 4. The *g* parameters are listed in Table 5. The NiCuNi complexes exhibit a broad weak

(29) Nakamoto, K. *Infrared and Raman Spectra of Inorganic and Coordination Compounds*, 5th ed.; John Wiley: New York, 1997; Part B.
(30) Güdel, H. In *Magneto-Structural Correlation in Exchange Coupled Systems*; Willet, R. D., Gatteschi, D., Kahn, O., Eds.; D. Reidel: Dordrecht, The Netherlands, 1985; p 297.
(31) Güdel, H. *Coord. Chem. Rev.* **1988**, *88*, 69.

band centered at approximately $g = 2.1$ and an intense broad signal with the maximum at about $g = 5.4$. The spin couplings in $Ni^{II}Cu^{II}Ni^{II}$ species give rise to two $S = {}^1/_2$, two $S = {}^3/_2$, and an $S = {}^5/_2$ states. The transition within the doublet state exhibits a resonance at a field corresponding approximately to $g = 2$. However, due to zero-field splitting effects, the allowed transitions within the quartet or sextuplet states will produce two resonant signals: one at the high field near $g = 2$ and the other at a low field with $g > 4$, assuming that the zero-field splitting is axial.[20,32] According to magnetic studies (vide infra), the energy gap $|5J/2|$ between the ground and highest excited states is ca. 250 cm^{-1}. This value is comparable to the kT value at room temperature (ca. 205 cm^{-1}), so all the spin states are thermally populated and make contributions to the observed broad signals.

The binuclear CuNi complex **5** also displays two resonance bands: one centered at $g = 2.20$ and the other at about $g = 5.55$. However, contrary to the NiCuNi species, the high-field signal is much more intense than the low-field band. This spectrum is due to the overlap of the signals of the $S = {}^1/_2$ and $S = {}^3/_2$ states. The doublet state resonates at about $g = 2$, while the quartet state presents two signals at about $g = 2$ and near the half-field, respectively.[32] Due to the antiferromagnetic nature of the interactions between Ni(II) and Cu(II) (vide infra), the ground state for the CuNi species is a doublet and that for NiCuNi species is a quartet. The ground state is the most populated and makes the largest contribution to the observed spectra. Therefore, the high-field signal for CuNi is more intense than the low-field one, and the opposite case occurs for NiCuNi (the high-field signal of the ground quartet state for NiCuNi is very weak[20]).

Magnetic Properties

NiCuNi Species. The spin-state structure of NiCuNi species has already been discussed by Kahn et al. It is irregular, that is, the energy of the low-lying states does not vary monotonically with spin. In the case in which the interaction between Ni(II) and Cu(II) is antiferromagnetic, the ground state is a quartet, above which there are two doublets, another quartet, and one sextuplet. Such an irregular spin-state structure is revealed by the $\chi_M T$ versus T plot, which exhibits a characteristic minimum. The $\chi_M T$ versus T plots for complexes **1**−**4** are shown in Figure 5. The $\chi_M T$ products at room temperature are about 2.2 cm^3 mol^{-1} K; they decrease smoothly upon cooling, reach the expected mimimum around 100 K with $\chi_M T$ at about 1.8 cm^3 mol^{-1} K, increase smoothly upon cooling further, and reach a maximum with $\chi_M T \approx 2.1$ cm^3 mol^{-1} K at ca. 16 K. After this maximum, the $\chi_M T$ values decrease rather rapidly. Such magnetic behavior at low temperature may be attributed to the zero-field splitting within the quartet ground state, which is confirmed by ESR spectra.

To simulate the experimental magnetic behavior, we used the following spin Hamiltonian that includes the ZFS parameter D of the ground state:

$$\hat{H} = -J(\hat{S}_{Ni1}\cdot\hat{S}_{Cu} + \hat{S}_{Ni2}\cdot\hat{S}_{Cu}) + D[\hat{S}_z^2 - {}^1/_3 S(S+1)] + \beta H[g_{Ni}(\hat{S}_{Ni1} + \hat{S}_{Ni2}) + g_{Cu}\hat{S}_{Cu}]$$

where the ZFS is assumed to be axial for simplicity. The expressions of the parallel and perpendicular magnetic susceptibilities deduced from the Hamiltonian are rather lengthy and have already been shown elsewhere.[20] Fitting the experimental data to the expressions leads to the parameters listed in Table 6. For comparative purpose, the parameters of three previously reported species containing hexacoordinated Ni(II) ions are also

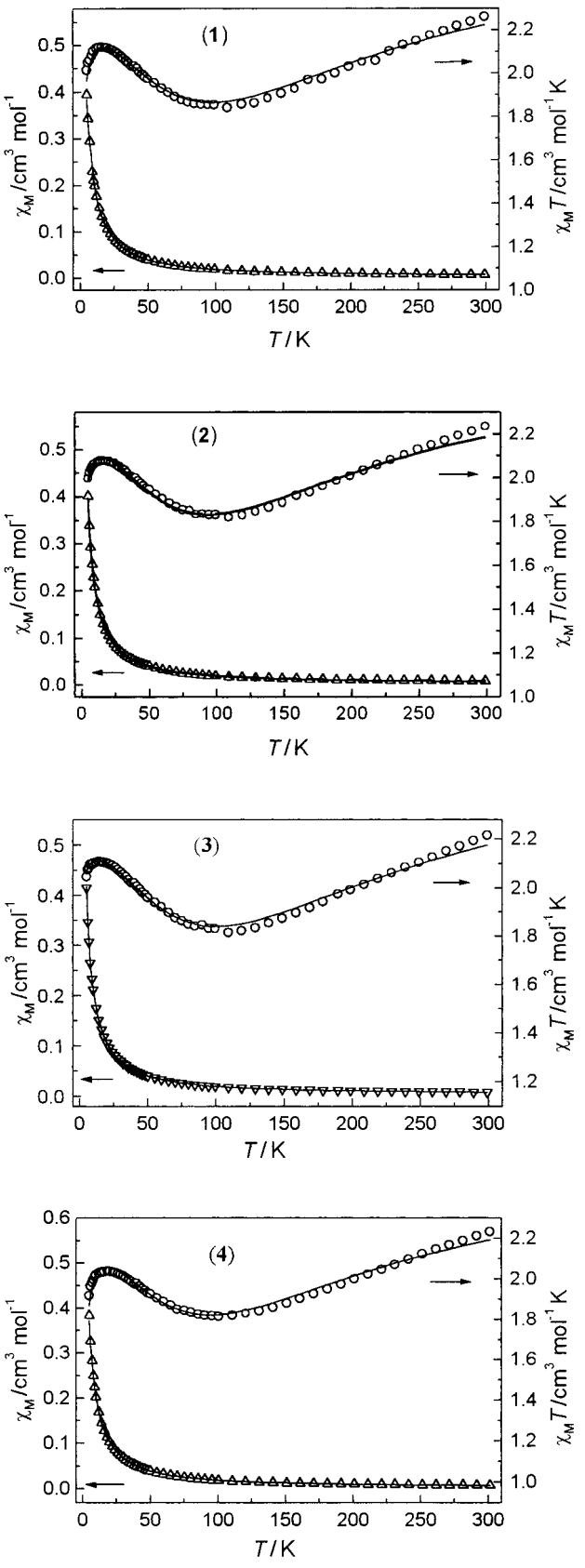

Figure 5. χ_M versus T and $\chi_M T$ versus T plots for the trinuclear species **1**−**4**.

(32) Escuer, A.; Vicente, R.; Ribas, J.; Costa, R.; Solans, X. *Inorg. Chem.* **1992**, *31*, 2627.

Table 6. Magnetic Parameters for Complexes **1**−**5** and Some Previously Reported Species

complex	J (cm^{-1})	g_{Ni}	g_{Cu}	D (cm^{-1})	R (10^{-5})	ref
{[Ni(bispictn)]$_2$Cu(pba)}$^{2+}$ (**1**)	−107.2	2.15	2.19	±3.3	7.1	this work
{[Ni(bispictn)]$_2$Cu(pbaOH)}$^{2+}$ (**2**)	−102.0	2.13	2.15	±2.7	4.6	this work
{[Ni(cth)]$_2$Cu(pba)}$^{2+}$ (**3**)	−109.2	2.13	2.15	±1.6	4.8	this work
	−124.5	2.24	2.18	±2.4	6.5	5
{[Ni(cth)]$_2$Cu(opba)}$^{2+}$ (**4**)	−104.2	2.13	2.18	±3.8	7.9	this work
{[Ni(bapa)(H$_2$O)]$_2$Cu(pba)}$^{2+}$	−90.3	2.19	2.12		350	6
{[Ni(cth)]$_2$Cu(pbaOH)}$^{2+}$	−90.0	2.20	2.29	±4.1	<100	20
{[Ni(cth)]$_2$Cu(Me$_2$pba)}$^{2+}$	−99.4	2.13	2.10	±8.3	<100	20
[Cu(opba)Ni(cth)] (**5**)	−108.0	2.23	2.19		19.6	this work

[a] $R = \Sigma(\chi_{obsd} - \chi_{calcd})^2/\Sigma\chi^2_{obsd}$.

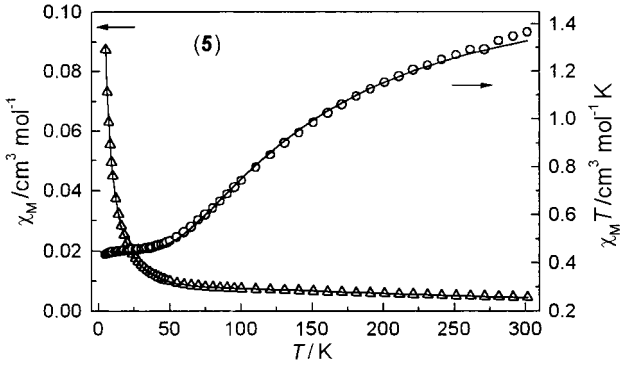

Figure 6. χ_M versus T and $\chi_M T$ versus T plots for the binuclear species **5**.

listed. It has been revealed that the N_2O_2 environment of the Cu(II) atom in {[Ni(bapa)(H$_2$O)]$_2$Cu(pba)}$^{2+}$ is markedly distorted from square planar toward tetrahedral, with deviations of the atoms from the mean plane being about ±0.2 Å,[6] much larger than those in **1** and **3**. This structural distortion may be responsible for the weaker antiferromagnetic interaction in {[Ni(bapa)(H$_2$O)]$_2$Cu(pba)}$^{2+}$.

NiCu Species. The $\chi_M T$ and χ_M versus T plots for complex **5** are shown in Figure 6. The $\chi_M T$ products at room temperature are about 1.3 cm^3 mol^{-1} K. They decreas smoothly upon cooling and reach a plateau below 35 K with $\chi_M T$ between 0.44 and 0.46 cm^3 mol^{-1} K. These features are typical of Cu(II)−Ni(II) pairs with antiferromagnetic intramolecular interaction. The plateau indicates that only the doublet ground state is thermally populated at low temperature.

On the basis of the isotropic spin Hamiltonian $\hat{\boldsymbol{H}} = -J\hat{\boldsymbol{S}}_{Cu}\cdot\hat{\boldsymbol{S}}_{Ni}$, the expression of the magnetic susceptibility for a CuNi pair is

$$\chi_M = \frac{N\beta^2}{4kT}\left[\frac{g_{1/2}^2 + 10g_{3/2}^2\exp(3J/2kT)}{1 + 2\exp(3J/2kT)}\right]$$

where the g_S ($S = {}^1/_2, {}^3/_2$) factors are related to local g factors by $g_{1/2} = (4g_{Ni} - g_{Cu})/3$, and $g_{3/2} = (2g_{Ni} + g_{Cu})/3$. The parameters obtained by the simulation of the experimental data using the above expression are also listed in Table 6. The J value is very close to those for NiCuNi species.

Acknowledgment. This work was supported by the Natural Science Foundation of China (No. 20071019 and No. 20071020).

Supporting Information Available: An X-ray crystallographic file in CIF format is available. This material is available free of charge via the Internet at http://pubs.acs.org.

IC001023H